arXiv:astro-ph/0609490v1 18 Sep 2006

Propagation of super high-energy cosmic rays in the Galaxy

Jörg R. Hörandel [a], Nikolai N. Kalmykov [b], and Aleksei V. Timokhin [c]

[a] *Institute for Experimental Nuclear Physics, University of Karlsruhe, P.O. Box 3640, 76021 Karlsruhe, Germany*

[b] *Skobeltsyn Institute of Nuclear Physics, Lomonosov Moscow State University, Leninskie Gory 1, Moscow, 119992 Russia*

[c] *Faculty of Physics, Lomonosov Moscow State University, Russia*

Abstract

The propagation of high-energy cosmic rays in the Galaxy is investigated. Solutions of a diffusion model are combined with numerically calculated trajectories of particles. The resulting escape path length and interaction path length are presented and energy spectra obtained at Earth are discussed. It is shown that the energy spectra for heavy elements should be flatter as compared to light ones due to nuclear interactions during the propagation process. The obtained propagation properties of ultra-heavy elements indicate that these elements could play an important role for the explanation of the second knee in the cosmic-ray energy spectrum around 400 PeV.

Key words: Cosmic rays; Propagation; Knee;
PACS: 96.50.S-, 96.50.sb, 98.70.Sa

1 Introduction

The explanation of the origin of super-high energy cosmic rays is one of the unsolved problems in astrophysics. The energy spectra at the sources are not identical to the observed spectra at Earth. Hence, studying the sources is closely related to investigations of cosmic-ray propagation processes in the Galaxy. For the latter, a detailed knowledge of the structure of the magnetic fields is important. Unfortunately, the configuration of the galactic magnetic field remains an open question — different models can explain the experimental data [1,2,3,4].

How cosmic rays are accelerated to extremely high energies is another unsolved problem. Although the popular model of cosmic-ray acceleration by shock waves in the expanding shells of supernovae (see e.g. [5,6,7]) is almost accepted as "standard theory," there are still serious difficulties. Furthermore, the question about other acceleration mechanisms is not quite

solved, and such mechanisms could lead to different cosmic-ray energy spectra at the sources [1].

Different concepts can be verified, calculating the primary cosmic-ray energy spectrum, making assumptions on the density of cosmic-ray sources, the energy spectrum at the sources, and the configuration of the galactic magnetic fields. The diffusion model may be used in the energy range $E < 10^{17}$ eV, where the energy spectrum is obtained using the diffusion equation for the density of cosmic rays in the Galaxy. At higher energies this model ceases to be valid, and it becomes necessary to carry out numerical calculations of particle trajectories for the propagation in the magnetic fields. This method works best for the highest energy particles, since the time required for the calculations is inversely proportional to the particle energy.

Therefore, a calculation of the cosmic-ray spectrum in the energy range $10^{14} - 10^{19}$ eV has been performed in a combined approach: solutions of a diffusion model are used at low energies and particle trajectories are numerically integrated at high energies.

In Sect. 2 the basic assumptions for the diffusion model will be described. The results obtained with the propagation model are presented in the subsequent sections. The calculated propagation path length and interaction probability of cosmic rays will be discussed in Sect. 3 and Sect. 4, respectively. Finally, the energy spectra are presented in Sect. 5, followed by a discussion of the results (Sect. 6).

2 Assumptions

High isotropy and a comparatively long retention of cosmic rays in the Galaxy ($\sim 10^7$ years for the disk model) reveal the diffusion nature of particle motion in the interstellar magnetic fields. This process is described by a corresponding diffusion tensor [1,3,8]. The steady-state diffusion equation for the cosmic-ray density $N(r)$ is (neglecting nuclear interactions and energy losses)

$$-\nabla_i D_{ij}(r) \nabla_j N(r) = Q(r). \quad (1)$$

$Q(r)$ is the cosmic-ray source term and $D_{ij}(r)$ the diffusion tensor.

Under the assumption of azimuthal symmetry and taking into account the predominance of the toroidal component of the magnetic field, eq. (1) is presented in cylindrical coordinates as

$$\left[-\frac{1}{r}\frac{\partial}{\partial r} r D_\perp \frac{\partial}{\partial r} - \frac{\partial}{\partial z} D_\perp \frac{\partial}{\partial z} - \frac{\partial}{\partial z} D_A \frac{\partial}{\partial r} + \frac{1}{r}\frac{\partial}{\partial r} r D_A \frac{\partial}{\partial z}\right] N(r,z) = Q(r,z) \quad (2)$$

where $N(r,z)$ is the cosmic-ray density averaged over the large-scale fluctuations with a characteristic scale $L \sim 100$ pc [3]. $D_\perp \propto E^m$ is the diffusion coefficient, where m is much less than one ($m \approx 0.2$), and $D_A \propto E$ the Hall diffusion coefficient. The influence of Hall diffusion becomes predominant at high energies ($> 10^{15}$ eV). The sharp enhancement of the diffusion coefficient leads to an excessive cosmic-ray leakage from the Galaxy at energies $E > 10^{17}$ eV. To investigate the cosmic-ray propagation at such energies it becomes necessary to calculate the trajectories for individual particles.

Such a numerical calculation of trajectories is based on the solution of the equation of motion for a charged particle in the magnetic field. The calculation was carried out using a fourth-order Runge-Kutta method. Trajectories of cosmic rays were calculated until they left the Galaxy. Testing the differential scheme used, it was found that the accuracy of the obtained trajectories for protons with an energy $E = 10^{15}$ eV after passing a distance of 1 pc amounts to $5 \cdot 10^{-8}$ pc. The retention time of a proton with such an energy averages to about 10 million years, hence, the total error for the trajectory approximation by the differential scheme is about 0.5 pc.

The magnetic field of the Galaxy consists of a large-scale regular and a chaotic, irregular component $\vec{B} = \vec{B}_{reg} + \vec{B}_{irr}$. A purely azimuthal magnetic field was assumed for the regular field

$$B_z = 0, \quad B_r = 0,$$
$$B_\phi = 1\ \mu\mathrm{G} \cdot \exp\left(-\frac{z^2}{z_0^2} - \frac{r^2}{r_0^2}\right), \qquad (3)$$

where $z_0 = 5$ kpc and $r_0 = 10$ kpc are constants [3]. These values are adopted from Ref. [3] to ensure the same conditions for both methods, i.e. trajectory calculations and the diffusion approach. The irregular field was constructed according to an algorithm used in [9], that takes into account the correlation of the magnetic field intensities in adjacent cells. The radius of the Galaxy is assumed to be 15 kpc and the galactic disk has a half-thickness of 200 pc. The position of the Solar system was defined at $r = 8.5$ kpc, $\phi = 0°$, and $z = 0$ kpc. A radial distribution of supernovae remnants along the galactic disk was considered as sources [10].

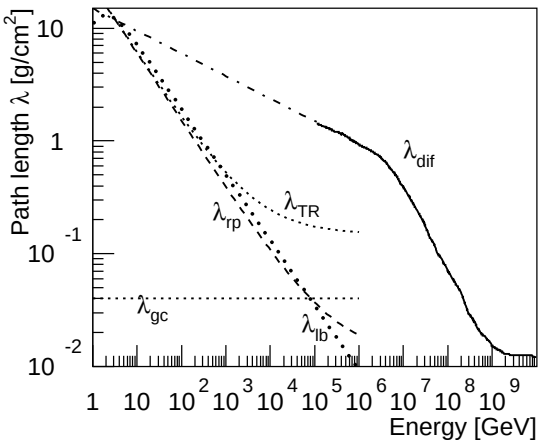

Fig. 1. Path length in the Galaxy for protons. The values for the diffusion model (λ_{dif}) are indicated by the solid line. They are extrapolated to lower energies by the dashed dotted line. Also shown are predictions of a leaky-box model (λ_{lb}, eq. (4)), a residual path length model (λ_{rp}, eq. (5)), and an upper limit for a residual path length model according to the TRACER experiment (λ_{TR}) [11]. The horizontal line indicates the matter to be passed along a straight line from the galactic center to the solar system (λ_{gc}).

3 Propagation Path Length

Assuming an interstellar matter density $n_d = 1$ cm^{-3} for the galactic disk and $n_h = 0.01$ cm^{-3} for the halo, following Chap. 3 in Ref. [1], trajectory calculations were performed at energies above 0.1 PeV. The dependence of the path length on energy was obtained from the dependence of the transport time for protons in the galactic disk and the halo. The resulting escape path length for protons as function of energy is presented in Fig. 1 as λ_{dif}. For heavier nuclei with charge Z the path length scales with rigidity, i.e. is related to the values for protons $\lambda^p(E)$ as $\lambda(E, Z) = \lambda^p(E/Z)$.

For protons at 4 PeV, the amount of tra-

versed material is approximately 0.7 g/cm^2. At higher energies, the calculated path length decreases as $\propto E^{-0.7}$. Between 0.1 and 1 PeV the calculations yield a behaviour $\lambda \propto E^{-\delta}$ with $\delta = 0.2$. The dashed dotted line indicates a trend below 0.1 PeV extrapolating the calculated values to lower energies using the slope obtained. This yields a path length around 15 g/cm^2 at 1 GeV, well compatible with measured values, see below. The relatively small $\delta = 0.2$ is much lower than the value usually assumed in Leaky-Box models ($\delta \approx 0.6$). On the other hand, such a slope of $\delta = 0.2$ follows from the diffusion model proposed in Ref. [3].

Measurements of the ratio of secondary to primary cosmic-ray nuclei at GeV energies are successfully described using a leaky-box model. For example, assuming the escape path length for particles with rigidity R and velocity $\beta = v/c$ as

$$\lambda_{lb} = \frac{26.7\beta \text{ g/cm}^2}{\left(\frac{\beta R}{1.0 \text{ GV}}\right)^{0.58} + \left(\frac{\beta R}{1.4 \text{ GV}}\right)^{-1.4}} \qquad (4)$$

various secondary to primary ratios, like boron to carbon, phosphorus to sulfur, and sub-iron to iron, as obtained by the ACE/CRIS and HEAO-3 experiments, can be described consistently in the energy range from $\sim$ 70 MeV to $\sim$ 30 GeV [12]. A similar approach is the residual path length model [13], assuming the relation

$$\lambda_{rp} = \left[6.0 \cdot \left(\frac{R}{10 \text{ GV}}\right)^{-0.6} + 0.013\right] \frac{\text{g}}{\text{cm}^2} \qquad (5)$$

for the escape path length. Recent measurements of the TRACER experiment yield an upper limit for the constant term in the residual path length model of 0.15 g/cm^2 [11]. The three examples are compared to the predictions of the diffusion model in Fig. 1.

Extrapolating these relations to higher energies leads to extremely small values at PeV energies due to the strong dependence of the path length on energy ($\propto E^{-0.6}$). For the approaches according to eq. (4) and eq. (5) above 10^5 GeV the traversed matter would be less than the matter passed along a straight line from the galactic center to the solar system $\lambda_{gc} = 8 \text{ kpc} \cdot 1 \text{ proton/cm}^3 \approx 0.04$ g/cm^2. This value is indicated in Fig. 1 as dotted line. For the upper limit obtained by TRACER the path length at 10^5 GeV amounts to about 0.17 g/cm^2. This value does not exclude diffusion, as the larmor radius $r_L = 1.08 \text{ pc} \cdot E[\text{PeV}]/(Z \cdot B[\mu\text{G}])$ of a proton with an energy of 0.1 PeV in the galactic magnetic field ($B = 1$ μG) is about 0.1 pc and 0.17 g/cm^2 correspond to about 34 pc or $340 r_L$ at 0.1 PeV. The value may be even larger when considering cosmic-ray propagation in the galactic halo. However, in this approach the cosmic-ray sources are expected to be closer to the solar system as in the diffusion model, since the latter yields a path length of about 1.5 g/cm^2 at 0.1 PeV. This value follows from the assumption that the sources are disributed like supernova remnants and, hence, the question may arise whether this assumption is true.

At low energies (GeV regime) the ratio of primary to secondary nuclei is measured to derive information about cosmic-ray propagation. At higher energies in the PeV domain such information is experimentally not accessible and other information is used to set constraints on propagation models. One possibility is the anisotropy of the arrival direction of cosmic rays. It can be characterized by Rayleigh ampli-

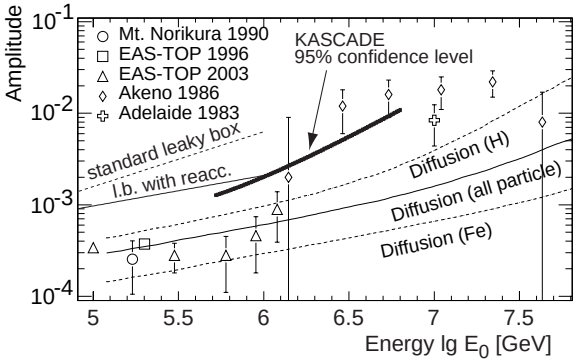

Fig. 2. Rayleigh amplitudes as function of energy for various experiments, taken from Ref. [14]. The results obtained by Mt. Norikura [15], EAS-TOP [16,17], Akeno [18], Adelaide [19], and KASCADE [14] are compared to predictions of leaky-box models [20] and a diffusion model [21]. For the diffusion model, predictions for primary protons, iron nuclei, and all particles are displayed.

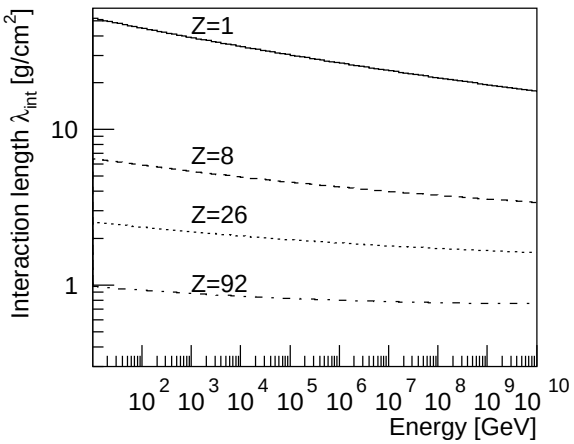

Fig. 3. Interaction length as function of energy for different elements based on cross-sections according to the hadronic interaction model QGSJET. The nuclear charge numbers are indicated.

tudes. Values observed by different experiments are compiled in Fig. 2 [14]. They are compared to predictions of propagation models. Two versions of a leaky-box model [20], with and without reacceleration are represented in the figure. Leaky-box models, with their extremely steep decrease of the path length as function of energy ($\lambda \propto E^{-0.6}$), yield relative large anisotropies even at modest energies below 10^6 GeV, which seem to be ruled out by the measurements, see also [20]. The measured values are almost an order of magnitude smaller. On the other hand, a diffusion model [21], which is based on the same basic idea [3] as the present work, predicts relatively small values at low energies and a modest rise only. In the figure, predictions for pure protons and iron nuclei are shown together with calculations for a mixed composition. The predicted Rayleigh amplitudes are compatible with the measured values. This may indicate, that diffusion models are a more realistic description of cosmic-ray propagation in the Galaxy at PeV energies.

4 Interaction Probability

To calculate the interaction length of nuclei in the interstellar medium, nuclear cross sections according to the hadronic interaction model QGSJET [22] have been used. The cross sections for nuclei with mass number $A > 1$ have been parameterized using

$$\sigma(E)[\mathrm{mb}] = \alpha(E) A^{\beta(E)}, \tag{6}$$

where α and β are approximated as

$$\alpha(E) = 50.44 - 7.93 \lg\left(\frac{E}{\mathrm{eV}}\right) + 0.61 \lg^2\left(\frac{E}{\mathrm{eV}}\right) \tag{7}$$

and

$$\beta(E) = 0.97 - 0.022 \lg\left(\frac{E}{\mathrm{eV}}\right). \tag{8}$$

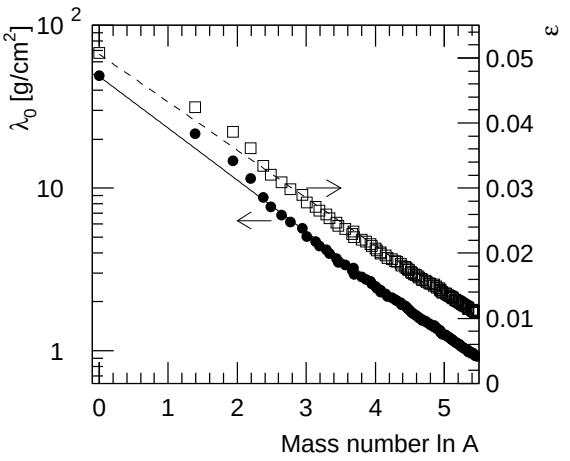

Fig. 4. Parameters λ_0 at 10 GeV (filled symbols, left scale) and ε (open symbols, right scale) to describe the interaction length as function of energy according to eq. (9) for nuclei with mass number A.

The corresponding interaction lengths for four different elements are presented in Fig. 3. The values decrease slightly as function of energy. Values for protons are in the range $55 - 20$ g/cm^2, the values decrease as function of nuclear charge and reach values < 1 g/cm^2 at all energies for the heaviest elements.

The dependence of the interaction length on energy has been approximated by the relation

$$\lambda_{int} = \lambda_0 \left(\frac{E}{10 \text{ GeV}} \right)^{-\varepsilon} . \qquad (9)$$

The corresponding values for all elements are depicted in Fig. 4 as function of the logarithm of the mass number A. The values for λ_0 at 10 GeV decrease from about 50 g/cm^2 for hydrogen to about 0.9 g/cm^2 for uranium. The small energy dependence is reflected in the values for ε ranging from 0.05 for protons to 0.01 for the heaviest element. The lines illustrate the approximately linear dependence of $\lg \lambda_0$ and ε on $\ln A$. Small deviations from this behavior

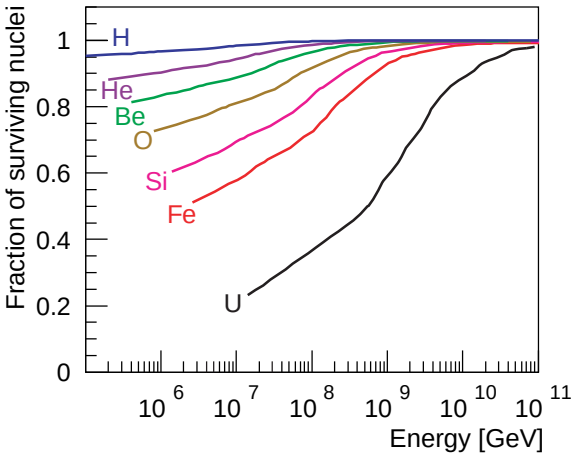

Fig. 5. Fraction of nuclei surviving without interaction in the Galaxy for different elements as function of energy.

are visible for the light elements helium, lithium, beryllium, and boron. The small values for ε motivate why λ_{int} is frequently assumed to be constant.

Using the path length λ_{dif} and the interaction length obtained, the interaction probability for different nuclei has been calculated. Nuclear fragmentation is taken into account in an approximate approach [23]. It should be pointed out that a nuclear fragment conserves the trajectory direction of its parent if Z/A in question is the same as for the primary nucleus and for most stable nuclei the ratio Z/A is close to 1/2. The resulting fraction of nuclei which survive without an interaction is presented in Fig. 5 for selected elements.

In the energy range shown protons reach the Earth almost undisturbed without any interaction, less than 5% of them interact. On the other hand, for heavier elements nuclear interactions play an important role and a significant fraction of them interacts at low energies. However, it turns out that even for ultra-heavy elements (heavier than iron) at the expected *knees* (at an energy of approximately $Z \cdot 4.5$ PeV), see below,

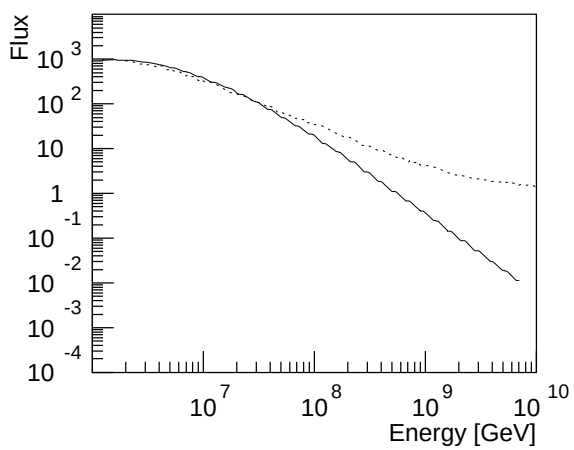

Fig. 6. Calculated spectra of protons for the diffusion model (solid line) and the numerical trajectory calculations (dotted line).

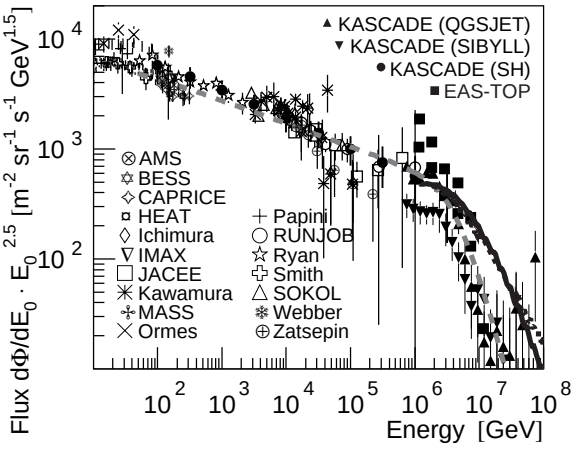

Fig. 7. Proton flux as obtained from various measurements, for references see [28], compared to the spectra shown in Fig. 6 (black lines) and the *poly-gonato* model [26] (grey, dashed line).

more than about 50% of the nuclei survive without interactions. This is an important result, which could help to understand the origin of the second *knee* in the all-particle spectrum around 400 PeV, as shall be discussed below. It should be noted that the fraction of surviving nuclei is even larger for a leaky-box model, with its low path length at such high energies.

5 Energy Spectra

The results for the calculations of the cosmic-ray proton spectrum are presented in Fig. 6. They were obtained using the diffusion model and numerical calculations of trajectories. It is evident from the graph that both methods give identical results up to about $3 \cdot 10^7$ GeV. At higher energies there is a continuous decrease of the intensity in the diffusion spectrum, which has its origin in the excessive increase in the diffusion coefficient that leads to large leakage of particles from the Galaxy.

An energy of 10^8 GeV can be taken as the conventional boundary to apply the diffusion model. At this energy the results obtained with the two methods differ by a factor of two and for higher energies the diffusion approximation becomes invalid.

Although the *knee* in the all-particle spectrum has been observed more than 40 years ago [24], it was only recently that experimental spectra for groups of elements became available. The KASCADE air shower experiment derived energy spectra for five groups of elements, namely protons, helium, CNO, silicon group, and iron group [25]. The spectra exhibit a fall-off for individual elements at high energies. These results and the data available from other experiments are compatible with the *poly-gonato* model [26], assuming a *knee* for each element at an energy of about $Z \cdot 4.5$ PeV [27].

In the following, we compare the predicted spectra already shown in Fig. 6 to direct and indirect measurements of the primary proton flux in Fig. 7. The predicted spectra are normalized to average experimental

values at 1 PeV. In the range depicted, almost no difference is seen between the two approaches. The relatively steep decrease of the measured flux at energies exceeding 4 PeV is not reflected by the predictions. On the other hand, the data are described reasonably well by the *poly-gonato* model [26], shown in the figure as well. The observed change in the spectral index $\Delta\gamma \approx 2.1$ according to the *poly-gonato* model has to be compared to the value predicted by the diffusion model. In the latter the change should be $1 - m \approx 0.8$ [3]. The observed value is obviously larger, which implies that the remaining change of the spectral shape should be caused by a change of the spectrum at the source, e.g. due to the maximum energy attained in the acceleration process.

The maximum energy and, therefore, the energy at which the spectrum steepens depends on the intensity of the magnetic fields in the acceleration zone and on a number of assumptions for the feedback of cosmic rays to the shock front. The uncertainty of the parameters yields variations in the maximum energy predicted by different models up to a factor of 100 [6,29]. It seems, there is no consensus about what the "standard model" is considered to predict. For the time being, it is difficult to draw definite conclusions from the comparison between the experimental spectra for different elemental groups and the "standard model" of cosmic-ray acceleration at ultra high energies.

6 Discussion

The energy spectra for individual elements measured at the Earth with GeV and TeV energies can be described by power laws $dN/dE \propto E^{\gamma}$ with values for the spectral index γ in the range -2.46 to -2.95 for elements from hydrogen to nickel [30,26]. The measurements seem to indicate that the steepness of the energy spectra at Earth depends on the mass of the nuclei, heavier elements seem to have flatter spectra. At higher energies in the PeV domain the measured spectra are compatible with the assumption of a *knee* for individual elements at about $Z \cdot 4.5$ PeV [26,27].

The energy spectrum of cosmic rays at their source $Q(E)$ is related to the observed values at Earth $N(E)$ as

$$N(E) \propto Q(E) \left(\frac{1}{\lambda_{esc}(E)} + \frac{1}{\lambda_{int}(E)} \right)^{-1} \quad (10)$$

with the escape path length λ_{esc} and the interaction length λ_{int}. Values for the former are presented in Fig. 1 and for the latter in Fig. 3. The relation between $N(E)$ and $Q(E)$ is governed by the absolute values of λ_{esc} and λ_{int} as well as their respective energy dependence. The interaction length λ_{int} is almost independent of energy, the values for ε in eq. (9) are smaller than 0.05, see Fig. 4. On the other hand, the propagation path length λ_{esc} decreases as function of energy as $\lambda_{esc} \propto E^{-\delta}$, with values between $\delta = 0.6$ for Leaky Box models and $\delta = 0.2$ for the diffusion model described in this work (see Sect. 3).

In the "standard picture" of galactic cosmic rays usually $\lambda_{int} > \lambda_{esc}$ is assumed with an energy independent interaction length and an escape path length $\lambda_{esc} = \lambda_{lb} \propto E^{-0.6}$. Thus, the relation between $N(E)$ and $Q(E)$ is dominated by the energy dependence of the escape path length. To explain the spectrum observed at Earth $N(E) \propto E^{-2.7}$ the spectrum at the sources has to be $Q(E) \propto E^{-2.1}$.

Recent measurements by the HESS experiment of the TeV gamma ray flux from the shell type supernova remnant RX J1713.7-3946 yield a spectral index $\gamma = -2.19 \pm 0.09 \pm 0.15$ [31]. For the first time, spectra have been derived directly at a potential cosmic-ray source. The results are compatible with a nonlinear kinetic theory of cosmic-ray acceleration in supernova remnants and imply that this supernova remnant is an effective source of nuclear cosmic rays, where about 10% of the mechanical explosion energy are converted into nuclear cosmic rays [32].

These investigations show that the spectrum at the source is $Q(E) \propto E^{-2.2}$, a value relatively close to the "standard model". The escape path length required to obtain the spectra observed at Earth should be $\propto E^{-0.5}$, i.e. δ is 0.1 smaller than in the "standard picture". Two questions remain open: Do all potential cosmic-ray sources exhibit a similar spectrum? And, what fraction of galactic cosmic rays is accelerated in supernova remnants with spectra like RX J1713?

Considering the spectra of nuclei observed at Earth, the second term in eq. (10) has to be taken into account. The values of λ_{int} for protons are at all energies larger than the escape path length λ_{dif}. Hence, for protons the escape from the Galaxy is the dominant process influencing the shape of the observed energy spectrum. For iron nuclei at low energies hadronic interactions are dominating ($\lambda_{int} \approx 2.5$ g/cm$^2 < \lambda_{dif}$) and leakage from the Galaxy becomes important only at energies approaching the iron *knee* ($26 \cdot \hat{E}_p$). Finally, for elements heavier than iron, the interaction path length is smaller than the escape path length at all energies, except above the respective *knees*. For these elements the propagation path length exceeds the interaction path length by about an order of magnitude at low energies. Hence, nuclear interaction processes are dominant for the shape of the observed spectrum. Taking this effect into account, it is expected that the energy spectra for heavy elements should be flatter as compared to light nuclei. The spectral index for iron nuclei should be about 0.13 smaller than the corresponding value for protons. Direct measurements indicate indeed that the spectra of light elements are flatter as compared to heavy elements [26], e.g. the values for protons $\gamma_p = 2.71$ and iron $\gamma_{Fe} = 2.59$ differ as expected. This more or less obvious effect has been pointed out earlier in several articles, see e.g. [33,34]. However, in the present work we extend the considerations to a wider energy range and ultra-heavy nuclei using contemporary estimates of the cross sections.

The *poly-gonato* model extrapolates results from direct measurements in the GeV and TeV regime to higher energies [26]. In the model fall-offs for individual elements proportional to the nuclear charge are assumed at energies of $E_Z = Z \cdot \hat{E}_p$, with the value $\hat{E}_p = 4.5$ PeV for protons. The *knee* is caused by the subsequential fall-offs for all elements, starting with protons. The second *knee* in the all-particle spectrum around 400 PeV is interpreted as the end of the galactic component, where the heaviest elements (actinides) reach their fall-off energies ($92 \cdot \hat{E}_p \approx 414$ PeV). At this energy, elements heavier than iron are expected to contribute with about 40% to the all-particle flux [35]. The model uses an empirical relation for the spectral index. The spectral slope decreases as function of nuclear charge. In the following, this behavior is investigated quantitatively with the propagation model discussed above.

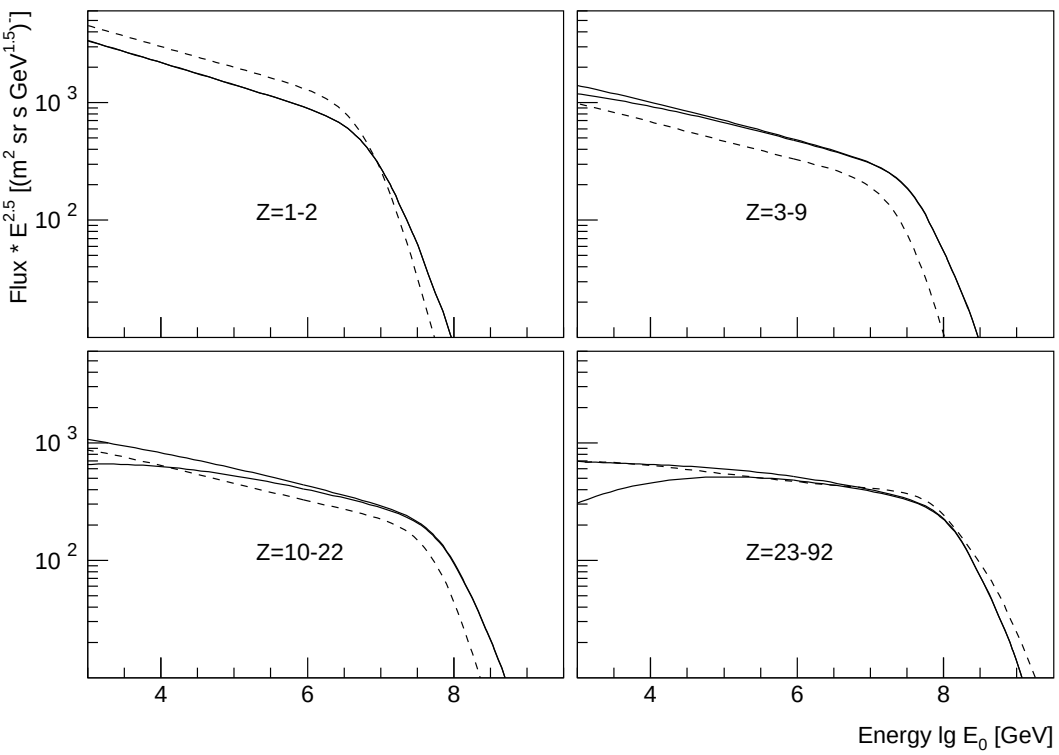

Fig. 8. Energy spectra at Earth for elements with nuclear charge Z as indicated. The dashed lines represent spectra according to the *poly-gonato* model, the solid lines are expected from the diffusion model discussed, see text. Two solid lines are shown in each panel, representing an estimate for the uncertainties.

As source composition, the abundances of elements from hydrogen to uranium as measured in the solar system [36] have been weighted with $Z^{3.2}$. This choice is arbitrary to a certain extent, but may be motivated by a higher efficiency in the injection or acceleration processes for nuclei with high charge numbers. The abundances are scaled with a factor which is identical for all elements to obtain approximately the absolute values as expected at the Earth according to the *poly-gonato* model. At the source, a power law $\propto E^{-2.5}$ has been assumed for all elements with a *knee*, caused e.g. by the maximum energy attained during the acceleration, at $Z \cdot 4.5$ PeV, with a power law index -3.5 above the respective *knee*. Using the derived propagation path length and interaction length, the amount of interacting particles has been determined. Secondary products generated in spallation processes are taken into account, assuming that the energy per nucleon is conserved in these reactions. They are added to the corresponding spectra with smaller Z. The spectra thus obtained are compared to spectra according to the *poly-gonato* model in Fig. 8.

Two features should be noted: The absolute fluxes at Earth are predicted quite well, especially when considering that only a simple scaling law has been introduced for the abundances at the sources, starting with the composition in the solar system. More important for the present discussion is the shape of the spectra. As expected, the shape of the proton spectrum is not influenced by the (few) interactions dur-

ing propagation and the difference of the spectral index at the source and at Earth $\gamma = -2.71$ [26] can be explained by the energy dependence of the escape path length $\propto E^{-0.2}$. On the other hand, it can be recognized that due to nuclear interactions the spectra for heavier elements are indeed flatter. The slopes obtained with the simple approach for the CNO, silicon, and iron groups agree well with the steepness as expected from the *poly-gonato* model. For heavy elements at low energies secondary products generated in spallation processes play an important role for the shape of the spectrum. At low energies many nuclei interact due to the large escape path length and the small interaction length, thus, the spectra of nuclei without any interaction deviate from power laws. However, the spallation products of heavier elements at higher energies compensate the effect and the resulting spectra are again approximately power laws, as can be seen in Fig. 8.

7 Summary

The results obtained show the effectiveness of the combined method to calculate the cosmic-ray spectrum using a numerical calculation of trajectories and a diffusion approximation. The propagation path length in the Galaxy and the energy spectra at Earth have been calculated to investigate the effect of escape from the Galaxy as possible origin of the *knee* in the cosmic-ray energy spectrum. The calculated dependence of the propagation path length on energy suggests difficulties with the "standard model" of galactic cosmic rays. An energy dependence of the propagation path length at low energies $\propto E^{-0.2}$ is expected, which requires a spectrum at the sources $\propto E^{-2.5}$ in order to explain the observed spectra at Earth. To explain the relatively steep fall-off of the observed energy spectra for elemental groups at their respective *knees*, the modulation of the spectrum due to propagation solely is not sufficient. An additional steepening of the spectra at the source is necessary, e.g. caused by the maximum energy attained during acceleration. It can be concluded that the *knee* in the energy spectrum of cosmic rays has its origin most likely in both, acceleration and propagation processes.

In the *poly-gonato* model the *knee* in the energy spectrum at $\hat{E}_p = 4.5$ PeV is caused by a cut-off of the light elements and the spectrum above the *knee* is determined by the subsequent cut-offs of all heavier elements at energies proportional to their nuclear charge number. The second *knee* around 400 PeV $\approx 92 \cdot \hat{E}_p$ is due to the cut-off of the heaviest elements in galactic cosmic rays. Considering the calculated escape path length and nuclear interaction length within the diffusion model, it seems to be reasonable that the spectra for heavy elements are flatter as compared to light elements. The calculations show also that even for the heaviest elements at the respective *knee* energies more than about 50% of the nuclei survive the propagation process without interactions. This may explain why ultra-heavy elements could contribute significantly ($\sim 40\%$) to the all-particle flux at energies around 400 PeV and thus explain the second knee in the energy spectrum.

Acknowledgments

The authors are grateful to J. Engler, A.I. Pavlov, and V.N. Zirakashvili for use-

ful discussions. N.N.K. and A.V.T. acknowledge the support of the RFBR (grant 05-02-16401).

References

[1] V. Berezinsky et al., Astrophysics of Cosmic Rays, North-Holland, 1990.

[2] A. Ruzmaikin et al., Magnetic Fields of Galaxies, Kluwer, Dordrecht, 1988.

[3] S. Ptuskin et al., Astron. & Astroph. 268 (1993) 726.

[4] E. Gorchakov, I. Kharchenko, Izv. RAN ser. phys. 64 (2000) 1457.

[5] D. Ellison et al., Astrophys. J. 488 (1997) 197.

[6] E. Berezhko, L. Ksenofontov, JETP 89 (1999) 391.

[7] L. Sveshnikova et al., Astron. & Astroph. 409 (2003) 799.

[8] N. Kalmykov, A. Pavlov, Proc. 26th Int. Cosmic Ray Conf., Salt Lake City 4 (1999) 263.

[9] V. Zirakashvili et al., Izv. RAN ser. phys. 59 (1995) 153.

[10] K. Kodaira, Publ. Astron. Soc. Japan 26 (1974) 255.

[11] D. Müller et al., Proc. 29th Int. Cosmic Ray Conf., Pune 3 (2005) 89.

[12] N. Yanasak et al., Astrophys. J. 563 (2001) 768.

[13] S. Swordy, Proc. 24th Int. Cosmic Ray Conf., Rome 2 (1995) 697.

[14] T. Antoni et al., Astrophys. J. 604 (2004) 687.

[15] K. Nagashima et al., Proc. 21st Int. Cosmic Ray Conf., Adelaide 3 (1990) 180.

[16] M. Aglietta et al., Astrophys. J. 470 (1996) 501.

[17] M. Aglietta et al., Proc. 28th Int. Cosmic Ray Conf., Tsukuba 4 (2003) 183.

[18] T. Kifune et al., J. Phys. G: Nucl. Part. Phys. 12 (1986) 129.

[19] P. Gerhardy, R. Clay, J. Phys. G: Nucl. Part. Phys. 9 (1983) 1279.

[20] V. Ptuskin, Adv. Space Res. 19 (1997) 697.

[21] J. Candia et al., J. Cosmol. Astropart. Phys. 5 (2003) 3.

[22] N. Kalmykov et al., Nucl. Phys. B (Proc. Suppl.) 52B (1997) 17.

[23] N. Kalmykov, S. Ostapchenko, Yad. Fiz. 56 (1993) 105.

[24] G. Kulikov, G. Khristiansen, JETP 35 (1958) 635.

[25] T. Antoni et al., Astropart. Phys. 24 (2005) 1.

[26] J.R. Hörandel, Astropart. Phys. 19 (2003) 193.

[27] J.R. Hörandel, astro-ph/0508014 (2005).

[28] J.R. Hörandel, astro-ph/0407554 (2004).

[29] J.R. Hörandel, Astropart. Phys. 21 (2004) 241.

[30] B. Wiebel-Soth et al., Astron. & Astroph. 330 (1998) 389.

[31] F. Aharonian et al., Nature 432 (2004) 75.

[32] H. Völk, E. Berezhko, astro-ph/0602177 (2006).

[33] P.L. Biermann et al., preprint astro-ph/0302201

[34] F.C. Jones et al., Astrophys. J. 547 (2001) 264

[35] J.R. Hörandel et al., astro-ph/0508015 (2005).

[36] A. Cameron, Space Sci. Rev. 15 (1973) 121.